Characterization and comparison of landslide triggering in different tectonic and climatic settings

L. Tatard,[1] J. R. Grasso,[1] A. Helmstetter,[1] and S. Garambois[1]

Received 8 December 2009; revised 3 August 2010; accepted 26 August 2010; published 29 December 2010.

[1] The spatial and temporal distributions of landslides in six catalogues are analyzed in order to better understand landslide triggering mechanisms. The six landslide catalogs are New Zealand, Yosemite (California), Grenoble (French Alps), Val d'Arly (French Alps), Australia, and Wollongong (New South Wales, Australia). Landslides are clustered in time for all catalogs. For New Zealand, Yosemite, Australia, and Wollongong, the frequency of landslides varies between 1 and 1000 events per day and is well fitted by a power law: there is no characteristic scale for daily rates. When the large rates of daily landslides are known to be rain or earthquake triggered, our results suggest the same triggering may hold for the small daily rates. Earthquakes are found to trigger landslides for the New Zealand, Yosemite, and Australia areas at distances as large as 20 times their fault lengths. There is no evidence of landslides triggered by earthquakes for the three other catalogs. Small $M \leq 4$ earthquakes have little influence on landslide triggering, if any, for all catalogs. For New Zealand, Yosemite, Val d'Arly, Australia, and Wollongong, the number of landslides per month is significantly correlated with monthly rainfall. A correlation with temperature is found only for Grenoble and New Zealand. Landslide triggering (strong clustering in time and space) is more important in New Zealand than in Grenoble, probably because the forcing (seismicity and climate) is stronger in New Zealand than in the French Alps but possibly also because of a high sensitivity to landslides in New Zealand. We suggest that intensity of clustering in space and time can be used to assess the importance of landslide triggering and the processes responsible for triggering.

Citation: Tatard, L., J. R. Grasso, A. Helmstetter, and S. Garambois (2010), Characterization and comparison of landslide triggering in different tectonic and climatic settings, *J. Geophys. Res.*, *115*, F04040, doi:10.1029/2009JF001624.

1. Introduction

[2] Our study focuses on the distribution of landslides in time and space in different tectonic, climatic and weathering conditions. For the two main landslide triggers, heavy rainfall and large nearby earthquakes, most past studies suggested the existence of empirical thresholds above which landslides can be triggered.

[3] For rainfall-triggered landslides, *Sidle and Ochiai* [2006] (modified from *Caine* [1980]) and *Crozier* [1999] found empirical relationships between the amount of rainfall and landsliding, depending on the antecedent water status of the soil. *Glade* [1998] established thresholds, ranging from 120 mm to 300 mm of daily rainfall, for which there is a probability of 100% to trigger a landslide in 3 parts of the North Island of New Zealand. Previous analyses of landslides triggered by rainfall have first shown that the thresholds are variable in space, depending on the susceptibility of a given landscape to rainfall [*Glade*, 2000; *Brooks et al.*, 2004]. Second, the thresholds for triggering seem to be variable in time, depending on the rainfall duration [*Guzzetti et al.*, 2007] and on the geomorphological stage of the slope [*Brooks et al.*, 2002; *Hufschmidt and Crozier*, 2008]. All these studies emphasize the complexity of the rainfall-landslide interactions [*Hufschmidt and Crozier*, 2008]. *Sandersen et al.* [1996] studied the seasonal occurrence of landslides in Norway and found that the yearly distribution of rock falls exhibits two maxima, one in early spring and one in late autumn. Both periods coincide with frequent fluctuations of temperature around the freezing point. The first maximum also coincides with the time of highest rate of snowmelt, while the second one coincides with the months of largest rainfall. *Gruner* [2008] and *Frayssines and Hantz* [2006] noticed an increase of rockfall events in the Alps during spring times, which underlines the influence of meteorological conditions such as frequent freeze-thaw cycles and snowmelt.

[4] Besides rainfall, the most common triggering mechanism of landslides is earthquakes [*Crozier*, 1996]. Based on a review of worldwide case studies, *Keefer* [1984, 2002]

[1]Laboratoire de Géophysique Interne et Tectonophysique (LGIT), Centre National de la Recherche Scientifique (CNRS), Université de Grenoble, Grenoble, France.

0148-0227/10/2009JF001624

reported that the minimum magnitude of a triggering earthquake was 4, and that the area A affected by landslides increases with magnitude M as $\mathrm{Log}_{10} A = M - c$ with $c = 3.46 \pm 0.47$. The area increases from $A = 0$ for $M = 4$ to $A = 500{,}000$ km^2 for $M = 9.2$. However, it should be noted that there is an extensive scatter around this general trend. The effect of small $M < 5$ earthquakes on landsliding has been less reported and studied than the effect of $M > 5$ earthquakes. The influence of $M < 5$ earthquakes on landslide initiation is ambiguous. *Del Gaudio et al.* [2000] found that the low-magnitude (maximum $M_L = 3.6$) earthquake sequence in Southern Italy only had an indirect influence on the 20 km distant Vadoncello landslide. *Sassa et al.* [2007] and *Walter and Joswig* [2008] argued for a possible triggering of the Leyte landslide (Philippines) and the Heumoes slope (Austria), respectively, by earthquakes with magnitude $2 < M_L < 3$ located between 10 and 20 km from the landslides. However, the Leyte landslide may also have been triggered by a heavy rainfall [*Sassa et al.*, 2007].

[5] In order to better understand landslide triggering in different tectonic and climatic settings, we analyze six catalogs of landslides: New Zealand landslides between 2001 and 2004, Yosemite (California, USA) between 1980 and 2004, cliffs in Chartreuse and Vercors massifs (French Alps near Grenoble) between 1982 and 2005, and in Val d'Arly (French Alps) between 1954 and 1975. We first analyze the distribution of landslides in time and space for these six areas. The influence of external forcing such as earthquakes and climate is then analyzed for each catalog, as well as possible interactions between landslides. Finally, we compare the importance of landslide triggering for all catalogs.

2. Databases

2.1. Landslide Databases

2.1.1. Description of the Databases

[6] The term "landslide" used in this study denotes all mass movements characterized by an episode of movement between quiet periods. It encompasses all falls, topples, slides, spreads and flows involving either rocks, debris or earth materials.

[7] The 1996–2004 New Zealand database was compiled by GNS Science Ltd and consists of 2100 events which occurred across the entire country. Data in the catalog were obtained from a variety of sources, such as media reports, aerial surveys and ground inspection [*Tatard*, 2010]. The 1857–2004 Yosemite database was compiled by USGS and consists of 519 events which occurred in the Yosemite National Park (California, USA) and surrounding areas. Data were obtained from review of published and unpublished historical accounts and field studies of recent rock falls [*Wieczorek and Snyder*, 2004]. The 1890–2005 Grenoble database was compiled by the Restauration des Terrains en Montagne office (RTM), a forestry office in charge of natural risks in the French Alps. The database consists of 144 events which occurred along the 120 km long Chartreuse and Vercors cliffs, in the vicinity of Grenoble (Isère, France) [*Dussauge et al.*, 2003]. The 1948–2000 Val d'Arly database consists of 221 landslides which occurred along a 16 km section of the D1212 road in the Val d'Arly (Haute-Savoie, France) and was compiled by the local road service. It has reported daily every event larger than 1 m^3 which had fallen on the road, causing road closure [*Dussauge et al.*, 2002]. The 1842–2007 Australia database was compiled by Geoscience Australia and consists of 965 events which occurred across the entire country. The 1890–2004 Wollongong database was compiled by the University of Wollongong and consists of 487 events which occurred along the 50 km long Illawarra escarpment, in the vicinity of Wollongong (New South Wales, Australia) [*Flentje and Chowdhury*, 2005; *Flentje et al.*, 2007].

[8] For each database, information on geology, type of movement and elevation is given in Table 1. Landslide time accuracy varies from 1 day to several months. Landslide location accuracy ranges from a few meters for GPS-located landslides to a few dozen kilometers for events remotely located using news reports, e.g., the distance to the nearest village. Some landslides have no location reported at all.

2.1.2. Selection of Robust Landslide Catalogs

[9] Only landslides with a time accuracy better than 2 days and a known location are selected for the analysis. Figure 1 illustrates the temporal evolution of the landslide rates and compares them with rainfall and seismicity rates in each area. In order to remove the influence of the large daily landslide clusters, a "binary catalog" is introduced (Figure 1). The daily binary rate is either equal to 1 (at least one landslide was reported in the catalog for this day) or 0 (no landslides were reported). The location of an event in the binary catalog is defined as the barycenter of all events that occurred during that day. It can be noted that there is an increase of the landslide binary rates with time for all catalogs except the Val d'Arly one. This increase can be due to (1) an improvement in data collection, (2) a change in the slope susceptibility, or (3) a change in the applied forcings. For the New Zealand and Wollongong databases, *Tatard* [2010] and *Flentje et al.* [2007] noted a change in the landslide collection after July 2001 and January 1988, respectively. However, the Yosemite, Grenoble and Australia time series display significant fluctuations which have not been related to any phenomenon, to our knowledge. As the rainfall and seismicity rates are relatively constant in time for all databases (Figure 1), it is more probable that the long-term (at least several years) unidentified changes in average landsliding rates are due to an improvement in data collection. For this reason, five out of the six catalogs were restricted to the most recent period, for which the binary landslide rates appears constant (Table 2 and Figure 2). These periods are July 2001–2004 for New Zealand, 1980–2004 for Yosemite, 1982–2005 for Grenoble, 1996–2007 for Australia and 1988–2000 for Wollongong. For the Val d'Arly catalog the 1954–1975 time period was chosen because stabilization works took place on the site after 1976, reducing the susceptibility of the slopes [*Dussauge et al.*, 2002]. Figure 3 gives the location of the selected landslides for all catalogs.

[10] Other available information in the databases sometimes includes volume and reported trigger (for New Zealand, Yosemite, Australia and Wollongong). The trigger mechanism relates to any nearby triggering event (intense rainfall or $M > 4$ earthquake) which occurred within 2 days from the landslides. Table 2 summarizes possible parameters that can be used to compare landslide triggering from one catalog to another. The parameters are mean landslide daily rate, landslide density (number of landslides per year and per square kilometer) and mean erosion (volume of the largest landslide

Table 1. Landslide Databases

	New Zealand[a]	Yosemite[b]	Grenoble[c]	Val d'Arly[d]	Australia[e]	Wollongong[e]
Date	1996–2004	1857–2004	1890–2005	1948–2000	1842–2007	1890–2004
Number of events	2100	519	144	221	965	487
Surface (km^2)	270,000	3000	3700	16	7,700,000	550
Geology	Heterogeneous	Granite	Limestone	Micashist	Heterogeneous	Sandstone, mudstone
Type of movement	Heterogeneous	Rockfalls rockslides	Rockfalls	Rockfalls	Heterogeneous	Heterogeneous
Elevation (m)	0–3800	1000–2300	250–1600	1000–1200	0–2200	300–500
Landslide with volume	13%	32%	35%	74%	9%	No data

[a]Database available at http://www.geonet.org.
[b]Database available at http://pubs.usgs.gov/of/2003/of03-491/.
[c]Characteristics of database from *Dussauge et al.* [2003].
[d]Characteristics of database from *Dussauge et al.* [2002].
[e]Database available at http://www.ga.gov.

normalized by the duration and the area for each catalog). All these values must be treated with caution since they were not corrected from their catalog resolution. Indeed, volume estimates for most catalogs are too imprecise (Table 1).

2.2. Earthquake Databases and Tectonic Settings

[11] Earthquake data are extracted from national catalogs (Table 3). Their magnitudes of completeness M_c, estimated using the *Ogata and Katsura* [1993] method, range from 1.9 to 3.0 (Table 3). The earthquake data represent different tectonic settings. Local seismicity was defined as seismicity located within the area covered by landslide catalog for New Zealand and Australia, and, for other catalogs, as seismicity located in a 300 km by 300 km box centered on the studied area. Table 3 gives the seismicity rate by year and by square kilometer for the 5 regions. New Zealand presents the strongest seismicity rate with on average 4.10^{-5} $M > 5$ earthquakes per year and per km^2. It is followed by California with on average 2.10^{-5} $M > 5$ earthquakes per year and per km^2. Due to intraplate tectonism, Wollongong experiences on average 9.10^{-7} $M > 5$ earthquakes per year and per km^2 while Australia has on average 4.10^{-7} $M > 5$ earthquakes per year and per km^2. Last, the French Alps experience 2.10^{-7} $M > 5$ earthquakes per year and per km^2. Figure 3 shows the 20 largest earthquakes for the analyzed time periods, for all catalogues but the Val d'Arly one (no earthquake $M > 2.2$ from 1954 to 1975 in this area). The contemporary tectonic uplift rate is the highest for New Zealand, ranging from 1 to 10 mm per year [*Fitzsimons and Veit*, 2001]. The South Island uplift is mainly localized along the Southern Alps, whereas the uplift in the North Island appears more diffuse, spreading and partitioning along dozens of major faults. The second highest uplift rate is found for the French Alps with 1 to 2 mm of uplift per year [*Fitzsimons and Veit*, 2001]. The Sierra Nevada block, of which the Yosemite is part, has uplift less than 1 mm/yr [*Dixon et al.*, 2000]. Finally, there is no contemporary uplift in Australia [*Miner et al.*, 2008].

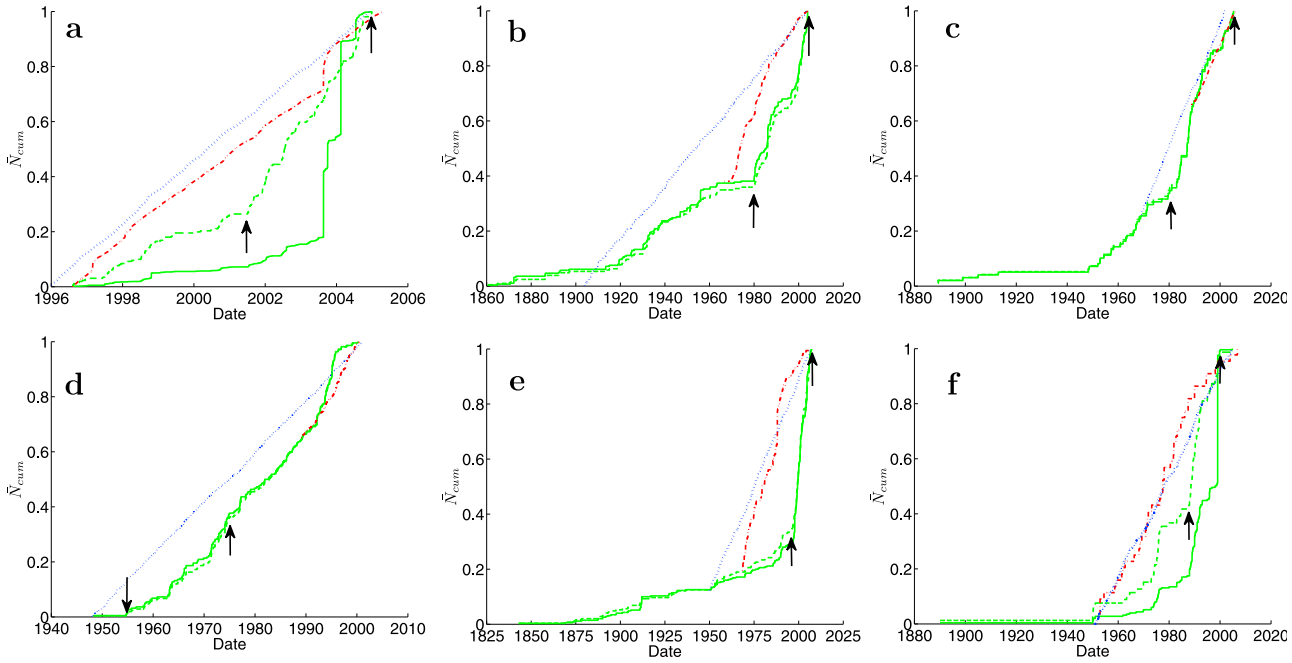

Figure 1. Normalized daily landslide rate, rainfall rate, and earthquake rate for the six databases: Entire (green solid line) and binary (green dashed line) landslide time series and rainfall (blue dotted line) and local seismicity (red dash-dotted line). (a) New Zealand, (b) Yosemite (c) Grenoble, (d) Val d'Arly, (e) Australia, and (f) Wollongong. Arrows indicate beginning and end of the catalogs extracted for this study.

Table 2. Selected Landslide Catalogs

	New Zealand	Yosemite	Grenoble	Val d'Arly	Australia	Wollongong
Date	July 2001–2004	1980–2004	1982–2005	1954–1975	1996–2007	1988–1999
N (events)	1788	172	63	83	247	207
N/T (events/d)	1.4	0.02	0.008	0.01	0.06	0.4
Density (events/yr/km^2)	1.9×10^{-3}	2.3×10^{-3}	7.0×10^{-4}	0.24	2.7×10^{-6}	0.03
V_{max} (m^3)	2.4×10^7	6×10^5	2×10^4	4×10^3	2×10^3	No data
Erosion rate of biggest event[a] (m^3/yr/km^2)	22	8	2.3×10^{-1}	11	2.7×10^{-5}	No data

[a]The erosion rate is equal to the maximum landslide volume V_{max} divided by catalog duration and by the spatial extent of the catalog.

2.3. Weather Databases and Climatic Settings

[12] As the landslide catalogs are analyzed as a whole, with no account taken of the local tectonic, geologic or climatic settings, we use global weather data, recorded over the same areas as the ones where landslides were recorded. We are aware that for New Zealand and Australia such strategy implies averaging data which have large variations, but this choice is coherent with the global analysis used for landslide databases.

[13] New Zealand's climate varies from warm subtropical conditions in the far north to cool temperate climate in the far south, with severe alpine conditions in the mountainous areas. Mountain chains extending over the length of New Zealand provide a barrier to the prevailing westerly winds, dividing the country into distinct climate regions (see *Whipple* [2009] for a discussion on the interaction between climate and tectonics in New Zealand). The West Coast of the South Island is the wettest area of New Zealand, whereas the area to the east of the mountains (100 km away) is the driest. Most areas of New Zealand record between 600 and 1600 mm of rainfall per year. Over the northern and central areas of New Zealand more rain falls in winter than in summer, whereas for much of the southern part of New Zealand, winter is the season of least rainfall (Data available at http://www.niwa.co.nz/education-and-training/schools/resources/climate/overview, September 2009).

[14] Australia is a large island continent with different climate zones, varying from tropical in the north through the arid expanses of the interior to temperate regions in the south. Seasonal fluctuations can be large, with temperatures ranging from above 50°C to well below zero. Minimum temperatures are moderated by the lack of mountains and by the influence of surrounding oceans. Australia is relatively arid, with 80% of the land recording less than 600 millimeters rain per year and 50% having less than 300 mm (Data available at http://wwww.bom.gov.au/lam/climate/levelthree/ausclim/ausclim.htm). Rainfall is highly seasonal and occurs mainly during summer.

[15] The climatic conditions of the Chartreuse and Vercors areas, near Grenoble, in the French Alps foothills, are characterized by wet spring (up to 90 mm/month) and fall (up to 110 mm/month) seasons. Val d'Arly area, located in the more central part of the French Alps, has wet summers with rainfall depth up to 240 mm/month. The climatic conditions of the Yosemite Park are a dry April–October period and wet October–April period (up to 180 mm/month). These three areas have cold winters with minimum monthly temperatures below 0°C.

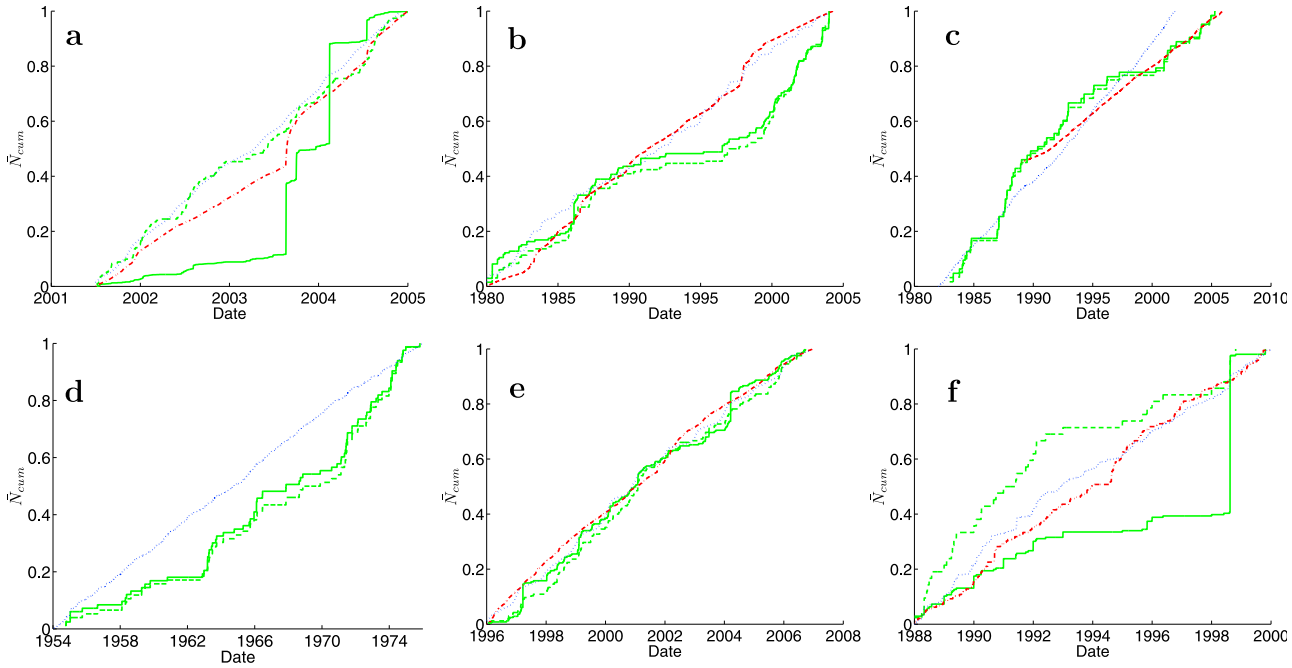

Figure 2. Same as Figure 1 after selecting the time interval when landslide rate is roughly constant, shown between arrows in Figure 1.

Table 3. Earthquake Catalogs[a]

	New Zealand[b]	Yosemite[c]	Alps[d]	Australia[e]	Wollongong[e]
Date	1996–2004	1965–2004	1989–2005	1950–2006	1950–2000
M_c	3.0 ± 0.03	1.9 ± 0.01	2.2 ± 0.1	2.5 ± 0.05	2.5 ± 0.05
M_{max}	7.1	7.0	4.8	6.9	5.8
$M > 5$/yr	12	2	0.05	3	0.14
$M > 5$/yr/km^2	4.10^{-5}	2.10^{-5}	2.10^{-7}	4.10^{-7}	9.10^{-7}

[a]Values are given for the whole country for New Zealand and Australia and for a box of 300 × 300 km^2 square centered on the studied area for Yosemite, Grenoble, Val d'Arly, and Wollongong areas.
[b]Database available at http://magma.geonet.org.
[c]Database available at http://www.ncedc.org.
[d]Database from Thouvenot (personal communication, 2008).
[e]Database from *Leonard* [2008].

[16] The New Zealand and Australia weather databases used in this study are averaged from hundred of gauges spread over the whole countries (Data available at http://www.niwa.co.nz/education-and-training/schools/resources/climate/overview and http://www.bom.gov.au/lam/climate/levelthree/ausclim/ausclim.htm, respectively). The Yosemite, Grenoble and Wollongong gauges are located within the three studied areas, whereas the Val d'Arly gauge is located 30 km to the North. The gauges were selected based on availability and completeness criteria for both rainfall and temperature data. For these local catalogs, the gauges give a robust estimate of local rainfall, whereas the estimate of temperature may be biased due to elevation differences between available gauges and landslides (largest offsets for Yosemite, Grenoble, Val d'Arly and Wollongong gauges are 1100 m, 1300 m, 200 m and 400 m, respectively).

[17] The New Zealand, Grenoble, Val d'Arly and Wollongong weather catalogs all show 10–15 rain days per month, all year long. The monthly rainfall depth is the key parameter that drives the differences between the six areas. New Zealand presents the largest amount of rainfall per month, up to 220 mm, followed by Yosemite and Wollongong, while Australia presents the smallest annual mean. Yosemite presents the greatest contrast between the minimum and maximum monthly rainfall depth (180 mm), while Grenoble presents the smallest contrast (40 mm) (see Table 4 for yearly data and Figure 4 for times series of rainfall).

3. Correlation Among Landslide Occurrences

3.1. Evidences for Inter-relationship Among Landslide Patterns and Rainfall and Seismicity

[18] All catalogs show clusters of landslides in time and space (Figures 3 and 4). Landslide clusters display different intensities, as measured by the number of landslides per cluster, and different spatial extents, as measured by the cluster size. These clusters are either associated with earthquakes (New Zealand), or large rainfalls (New Zealand, Yosemite, Australia, Wollongong) or with neither earthquake nor large rainfall. No simple interaction between landslides and either rainfall or earthquakes can be deduced from Figures 3 and 4 since similar forcings seem to produce very variable responses. For example, looking at the three largest rainfall in Wollongong, one triggered more than one hundred landslides in 1 day while the two other rainfall events only triggered a few landslides. To understand these observations, we analyze the distribution of landslides in time, and the spatiotemporal correlations between landslides. In a second step, we study the influence of external forcings (climate and earthquakes) on landslide triggering.

3.2. Landslide Daily Patterns

[19] The landsliding rates of the New Zealand, Yosemite, Australia and Wollongong catalogs show a larger variability than both their rainfall and seismicity counterparts (Figure 1). The peak value of daily landslide rates varies over 2 orders of magnitude: from 1 and 3 landslides per day for Grenoble and Val d'Arly, up to 10 for Yosemite and Australia and more than 100 for New Zealand and Wollongong. For all catalogs, daily rates larger than three events per day correspond in the databases to landslides reported as either rain triggered (New Zealand, Wollongong, Australia, Yosemite) or earthquake triggered (New Zealand, Yosemite).

[20] The mean daily rates range between 0.01 events per day for Grenoble and 1.4 events per day for New Zealand (Table 2). The landslide densities span 5 orders of magnitude, from 2.7 10^{-6} events/yr/km^2 for Australia to 2.4 10^{-1} events/yr/km^2 for Val d'Arly. The largest and smallest landslide daily rates do not correspond to the largest and smallest landslide densities. These patterns emphasize the scale effect inherent to our choice of catalogs. As an example, Val d'Arly is an active cliff extending over a 10 km scale, while New Zealand is an active mountain range extending over a 1000 km scale. Landslide recording is therefore very different between one catalog and another and the landslide rates and densities should be normalized by the resolution of each landslide catalog (as performed for earthquake catalogs [e.g., *Traversa and Grasso*, 2009]). The detection threshold V_0 is usually defined by fitting a power law distribution to the cumulative volume distribution and looking at the deviation from a power law for small volumes [e.g., *Dussauge et al.*, 2003]. Because volume estimates are reported for less than 40% of events for most catalogs (Table 1), V_0 values cannot be calculated for all catalogs and therefore the landslide rate and density values cannot be corrected from the catalog resolution. Accordingly, landslide rates and densities in Table 2 must not be over interpreted. These results emphasize the difficulty of establishing accurate indices from available catalogs, in the absence of better volume estimates, which inhibit comparisons between different landslide catalogs. In order to do so, we transfer tools used to analyze other natural complex systems such as earthquakes and volcanic eruptions, to analyze landslide triggering.

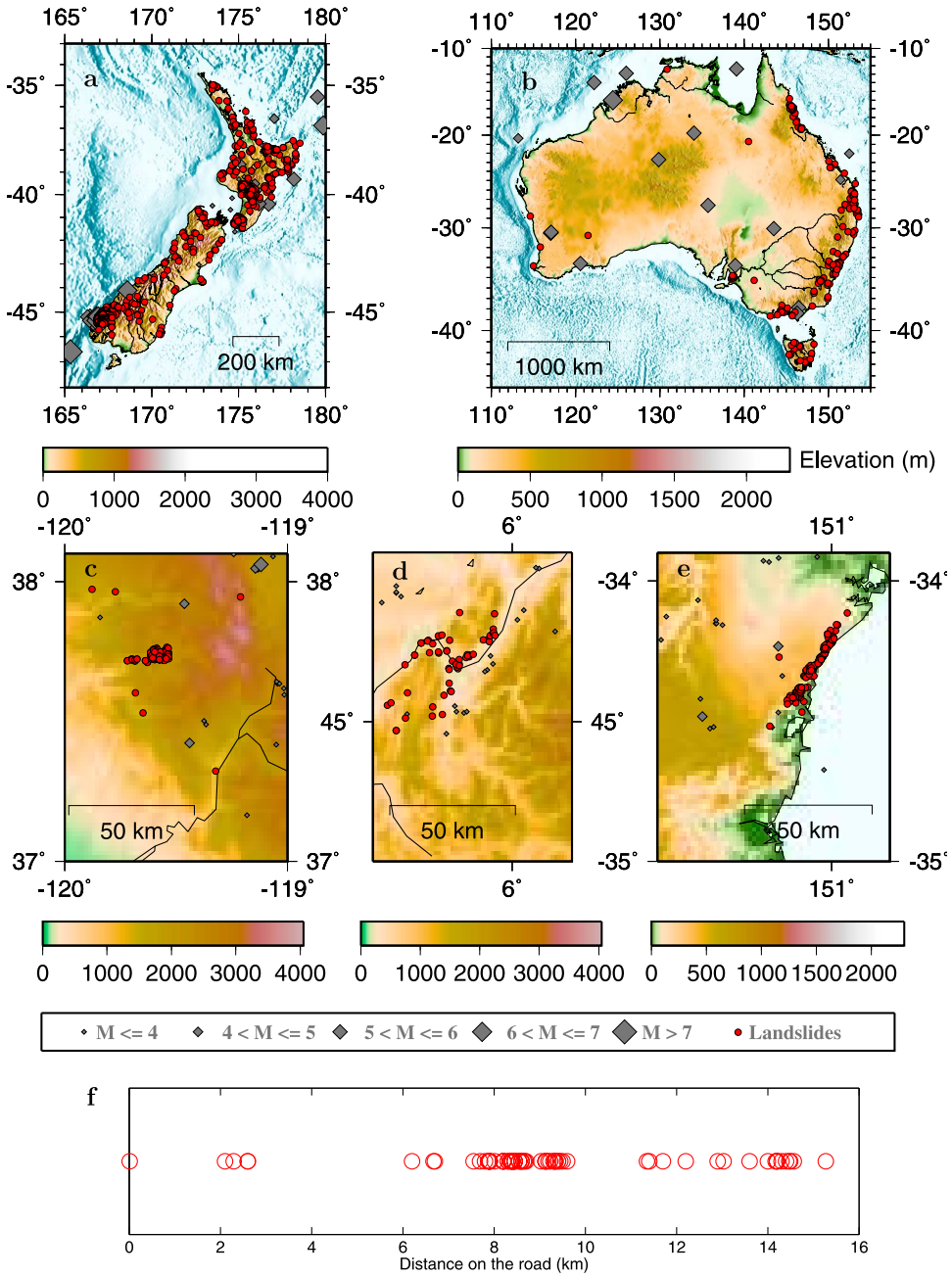

Figure 3. Landslide locations (red dots), 20 largest earthquakes (gray diamonds), in the selected box, and associated topography: (a) 1788 New Zealand landslides, (b) 247 Australia landslides, (c) 172 Yosemite landslides, (d) 63 Grenoble landslides, (e) 207 Wollongong landslides, and (f) 83 Val d'Arly landslides.

3.3. Distribution of Landslide Times and Waiting Times

[21] Clustering or periodicity of events in time can be characterized by the ratio η between the standard deviation of inter-event times dt and the average value of dt [e.g., *Marzocchi and Zaccarelli*, 2006]. For a Poisson process, i.e., a uniform distribution in time, $\eta = 1$, and the distribution of inter-event times obeys an exponential distribution. $\eta > 1$ characterizes events that are more clustered than a Poisson process, while $\eta < 1$ is typical for more regular occurrence times. The assumption that occurrence times obey a Poisson process is rejected for all areas, for both the full and binary catalogs, using the η test (Table 5). The entire Grenoble and Val d'Arly catalogs are characterized by the smallest η values and therefore are the less clustered in time, whereas the entire New Zealand catalog appears to be the most clustered. To further investigate clustering of landslides in time, the waiting time distributions for the six catalogs are analyzed (Figure 5). For each catalog, there is a threshold time (t_r) above which large inter-event times are more frequent than expected from an exponential distribution (Figure 5). t_r ranges between

Table 4. Rainfall and Temperature for the Six Studied Areas

	New Zealand[a]	Yosemite[b]	Grenoble[c]	Val d'Arly[c]	Australia[d]	Wollongong[d]
Rainfall monthly min–max[e] (mm)	90–220	0–180	65–105	75–145	15–100	65–160
Rainfall annual mean (mm)	150	80	85	105	45	115
Rain days per month[e]	10–16	No data	10–16	10–15	No data	8–15
Monthly min–max T[e] (°C)	1–22	−2–32	−1–29	−8–22	15–28	8–26

[a]Database from National Institute of Water and Atmospheric Research (NIWA), New Zealand.
[b]Database from National Climatic Data Center, USA.
[c]Database from Météofrance.
[d]Database available at http://www.bom.gov.au/.
[e]Monthly minima and maxima were obtained by averaging, per month, over the time period of the corresponding landslide catalog, monthly weather variables, in order to get the yearly climatic trend of the studied area.

30 and 250 days (Table 5). This deviation from a Poisson process for $t > t_r$ may be due to seasonal variations of climate, because landslides are less frequent during the dry season.

3.4. Distribution of Landslide Daily Rates

[22] To further constrain landslide occurrences, we analyze the distribution of daily rates (Figure 6). The heavy tail of the distributions suggests fitting these distributions by a power law. The method of *Clauset et al.* [2009] based on the Maximum Likelihood Method [*Aki*, 1965] is used to evaluate the power law exponent, along with the Kolmogorov-Smirnoff test [e.g., *Press et al.*, 1992] to test the power law goodness-of-fit. The New Zealand, Yosemite, Australia and Wollongong daily rates accept a power law distribution (Table 6) for daily rates larger than 1 event/day. This result implies that there is no characteristic scale for daily rates. The Grenoble and Val d'Arly catalogs present only 3 and 8 days, respectively, with more than one landslide per day, and the power law fit is rejected (Table 6 and Figure 6). For New Zealand, Australia and possibly Wollongong, there is a change in slope for daily rates larger than 10–20 events per day: the frequencies of the empirical daily rates are larger than expected from the best fit power law (Figure 6). This suggests either a different origin or mechanism for the largest landslide clusters or a bias in the sampling. Indeed, there may be an oversampling of the large clusters, for which a precise reconnaissance is often set up in order to map the landslides.

3.5. Distribution of Landslide Inter-event Distances

[23] After analyzing clustering of landslides in the time domain, we consider the distribution of landslides in space and its evolution with time. The distribution of inter-event distances is first evaluated using all couples of events in the catalog, and then selecting only events occurring on the same day, or with an inter-event time dt of 1 day. All distributions are normalized by the maximum time lag between events, so that all curves would overlap if there were no correlations between landslide locations and times. The distributions are computed using a lognormal kernel [e.g., *Izenman*, 1991]. A location error 0.01 km and 1 km was added to Val d'Arly distances and to New Zealand, Yosemite, Grenoble, Australia and Wollongong distances, respectively.

[24] Figure 7 compares the average inter-event distance distribution for $dt > 1$ day to the distribution obtained for $dt = 0$. Figure 8 presents the same analysis for the binary catalogs, comparing the case $dt = 1$ with $dt > 1$. The difference between the two curves in each plot highlights (1) the intensity of landslide triggering for a given time delay dt and (2) the distance range where landslides were triggered (Figures 7 and 8).

[25] All catalogs show a significant triggering for $dt = 0$ (Figure 7). For $dt = 1$ day, significant triggering is found only for New Zealand, Yosemite and Australia catalogs (Figure 8). At $dt = 0$ day, landslide triggering is maximum for distances smaller than 50 km and extends up to 200 km for New Zealand. Landslide triggering is maximum for distances smaller than 30 km and extends up to 400 km for Australia. This distance corresponds to the size of the sampled area for Yosemite, Val d'Arly and Wollongong catalogs. Note that for Grenoble and Val d'Arly, there are only a few landslides occurring on the same day, therefore this distance is not well constrained. The triggering observed for $dt = 0$ is not only driven by the largest landslide clusters: we still observe triggering after removing from the catalogs the clusters with more than one hundred events per day. For $dt = 1$ day, the spatial extent of landslide triggering is roughly similar to the size of the sampled area for New Zealand and Australia, while it is close to 10 km for Yosemite. The values of the triggering distances for $dt = 0$ and $dt = 1$ are a measure of the combined effect of the trigger intensity and of the slope susceptibility for each area.

4. Analysis of the Possible Processes for Landslide Triggering

4.1. Landslide-Landslide Interactions

[26] The distribution of the inter-event distances analyzed in section 3 showed that there are more landslides than expected within the same day or the day following a landslide occurrence (Figures 7 and 8). The inter-event distance distributions show that most of these landslides are within 50 km of each other. These distances are too large to result from landslide-landslide interactions. This correlation could be driven by the primary trigger itself. For the weather trigger, the correlation can be due to the residence or transit time of the weather event. For the earthquake trigger, aftershocks are the best candidate to explain the time delay between events and the inter-event distance (see also section 4.2).

[27] In order to analyze interactions between landslides, we analyze the landslide rate before and after the 10 largest landslides of New Zealand, Yosemite, Grenoble, Val d'Arly and Australia, where robust volume data are available. In order to do so, landslide time series of the binary catalogs are stacked relative to the time of each of these 10 large events, in order to increase the signal to noise ratio [e.g., *Lemarchand and Grasso*, 2007; *Tatard*, 2010]. For New Zealand, there are more landslides in a 20 day period after

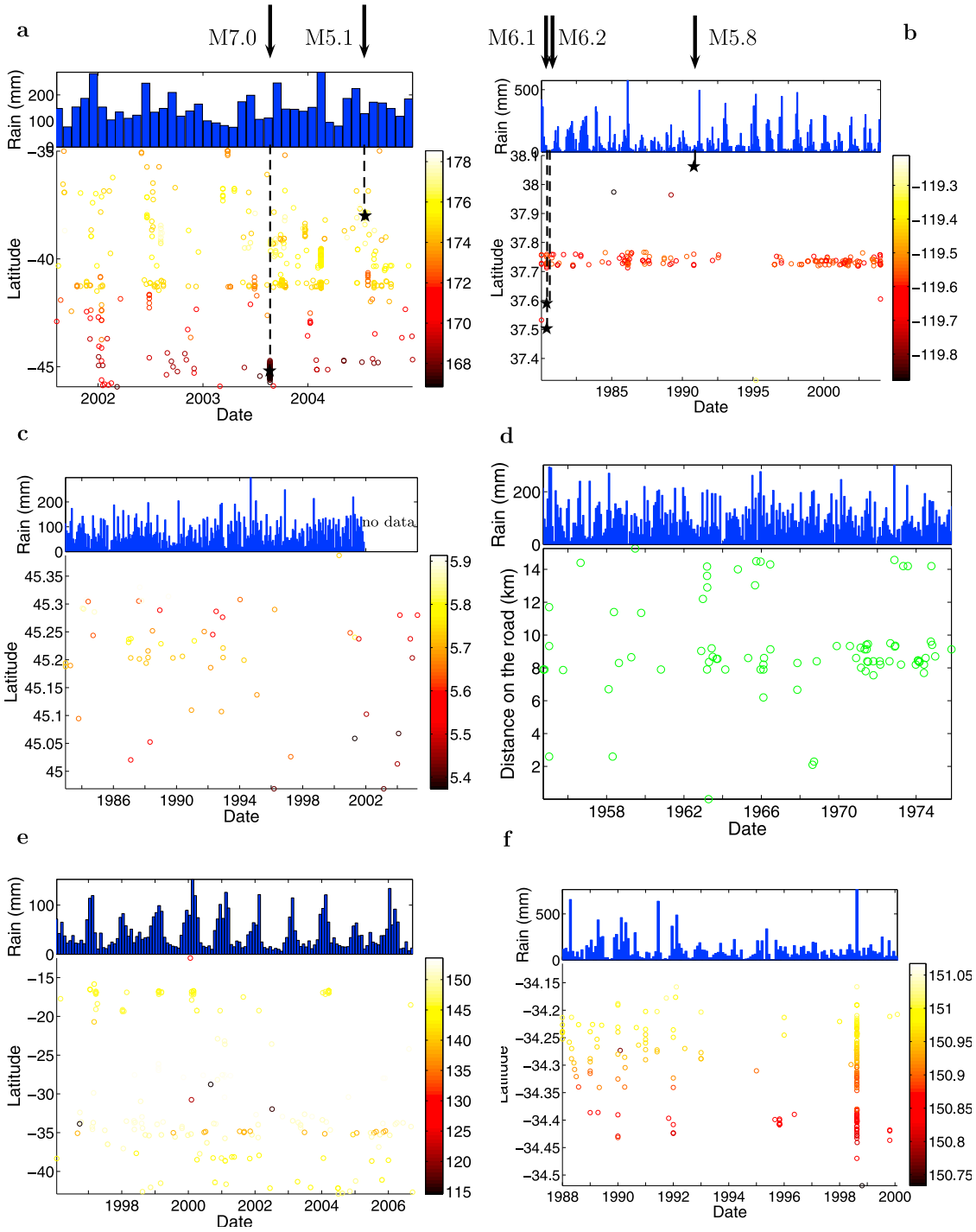

Figure 4. Space-time diagrams for landslide activity: landslides (circles) as a function of space (y axis for latitude and color for longitude) and time. The upper blue histogram gives monthly rainfalls (mm). The black arrows and black stars (New Zealand and Yosemite) give the location of the earthquakes which were reported in the catalog as having triggered landslides. (a) New Zealand, (b) Yosemite, (c) Grenoble, (d) Val d'Arly, (e) Australia, and (f) Wollongong. Figure 4d y axis corresponds to distances (km) along the road-cut.

the large landslides than in the 20 day period before it (Figure 9). In contrast, for Grenoble and Val d'Arly there are more landslides during the 20 days before the large landslides than after (Figure 9). The Yosemite and Australia catalogs show a roughly similar landslide rate before and after the largest landslides. In order to check the significance of these patterns we apply the same method on randomized catalogs generated by randomly selecting ten landslides from the studied catalog. The probability of getting at least the same absolute deviation between the number of landslides in

Table 5. The η Test and t_r Values[a]

Catalog	N	η	t_r (days)
New Zealand	1788	2.3	1
New Zealand binary	192	1.5	30
Yosemite	172	2.1	100
Yosemite binary	132	1.8	180
Grenoble	63	1.2	250
Grenoble binary	60	1.2	250
Val d'Arly	83	1.5	150
Val d'Arly binary	76	1.4	100
Australia	247	1.8	25
Australia binary	163	1.3	50
Wollongong	207	3.4	1
Wollongong binary	44	1.3	250

[a]N is the number of landslides of the studied catalog; $\eta > 1$ characterizes distributions more clustered than a uniform one; $\eta = 1$ corresponds to a Poisson process, and $\eta < 1$ characterizes quasi-periodic events; and t_r is the inter-event time after which the distribution departs from the exponential function.

the 20 days before the large landslides and in the 20 days after the large landslides is less than 1%, 1% and 7% for New Zealand, Grenoble and Val d'Arly, respectively.

[28] The distances between the largest landslides and the landslides occurring 20 days before or after them are mostly larger than 1 km (Figure 10). However, there is also a cluster of nearby events occurring on the same day or 1 day before or after the large events for New Zealand, Yosemite and Australia. These events occurring very close to the largest landslides before them may be precursors, while those occurring after them may have been triggered by the large landslides.

[29] In summary, we found no systematic change in landslide triggering before and after large landslides as different catalogs display different behaviors. Further investigation is needed to establish the existence of precursors or interactions between landslides.

4.2. Earthquake-Landslide Interactions

[30] The possible triggering of landslides by earthquakes is analyzed by stacking time series of landslides relative to each earthquake time, in order to increase the signal-to-noise ratio, as performed for landslide-landslide interactions (see section 4.1).

[31] Seismicity is dominated by small-magnitude earthquakes, since they are much more numerous than larger earthquakes [*Gutenberg and Richter*, 1956]. In order to keep only the earthquakes which may have had an influence on landslide triggering, we select earthquakes within a distance Δ/L from landslides, following the method of *Lemarchand and Grasso* [2007]. Δ is the landslide-earthquake hypocenter distance and L is the fault length calculated from the earthquake magnitude [*Wells and Coppersmith*, 1994]. The complete landslide databases (Table 1) are used for this test. Earthquakes with a magnitude $M > M_c$ and not deeper than 200 km were selected for the time and space correlation to landslides. Further, we use declustered earthquake catalogs; that is, we removed the aftershocks which occurred within 2 days from $M > 4$ mainshocks at distances smaller than 10 times the ruptured fault length of the involved mainshock (10 times the ruptured fault is the distance at which mainshocks are found to trigger most aftershocks [*Felzer and Brodsky*, 2006]). Keeping aftershocks in the earthquake catalog would produce a spurious increase in landslide triggering before $t = 0$ day, while the landslides were more likely triggered by the previous largest earthquake (i.e., the mainshock).

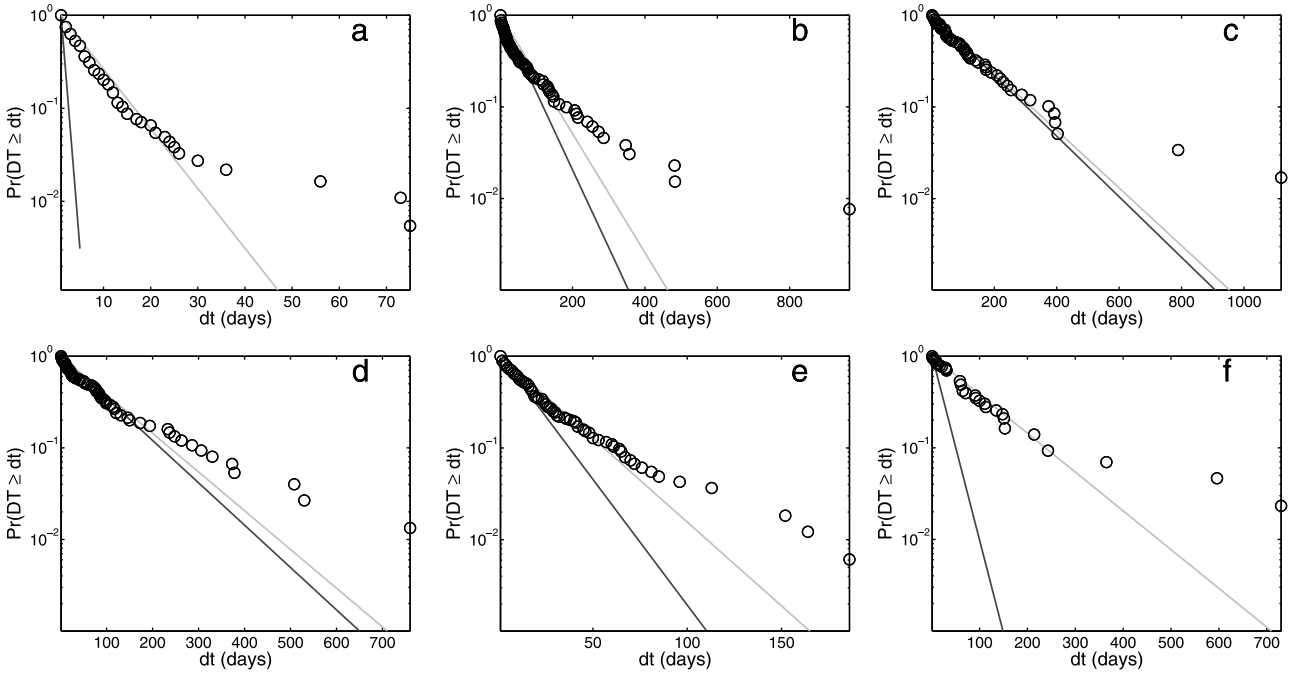

Figure 5. Cumulative distribution of landslide waiting times (circles) along with exponential distributions (corresponding to a uniform distribution of times) computed from the entire catalog (dark gray line) and from the binary landslide catalog (light gray line): (a) New Zealand, (b) Yosemite, (c) Grenoble, (d) Val d'Arly, (e) Australia, and (f) Wollongong.

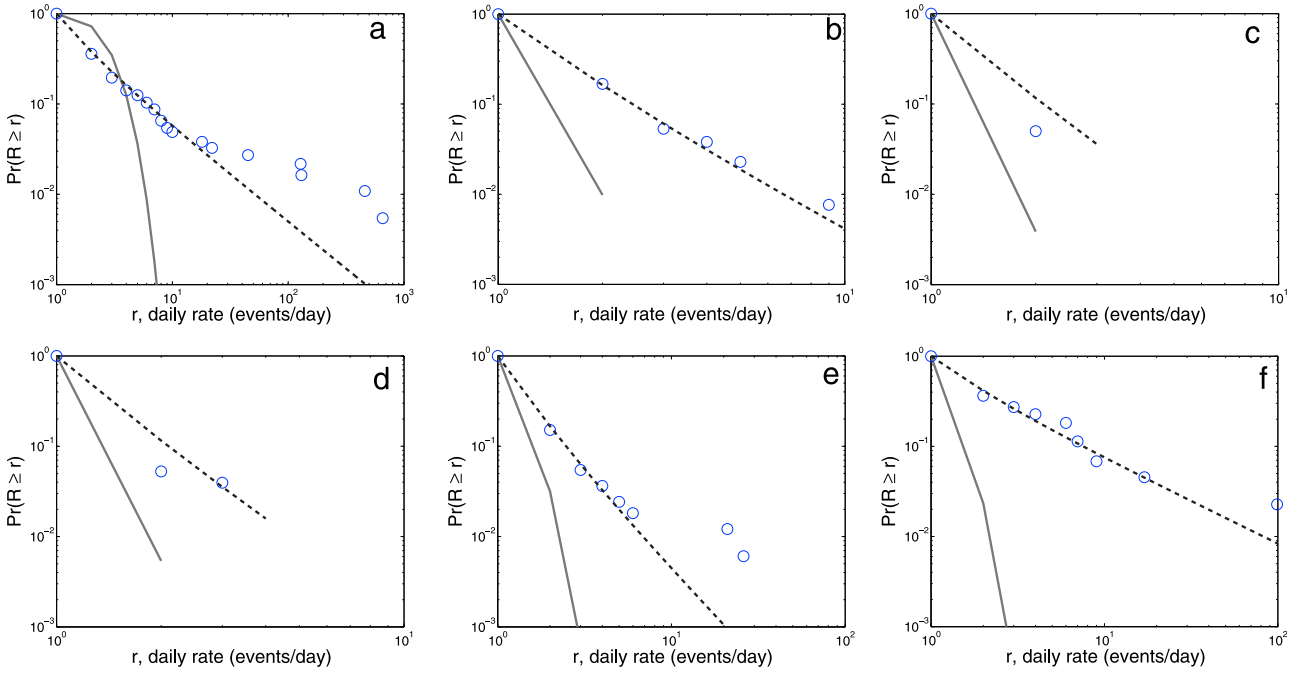

Figure 6. Cumulative distribution function (CDF) of landslide daily rates (circles); best Kolmogorov-Smirnoff power law fit (dashed line). (a) New Zealand landslides, (b) Yosemite landslides, (c) Grenoble cliffs landslides, (d) Val d'Arly cliff landslides, (e) Australia landslides, and (f) Wollongong landslides. The solid line represents the best fit exponential function. Values of exponent b and lower cutoffs are given in Table 6. Note that the fit is slightly curved for daily rates lower than 6 events/day, which is inherent to the definition of a discrete power law [e.g., *Clauset et al.*, 2009] and that the exponent of the CDF B is equal to $b-1$ [e.g., *Bonnet et al.*, 2001].

[32] We find an increase in landslide rate for landslides occurring within $t = -1$ to $t = 2$ days after earthquake occurrences for New Zealand, Yosemite and Australia (Figure 11) and no increase in landslide rate for Grenoble, Val d'Arly and Wollongong. Note that this timing (−1 to 2 days) also corresponds to the error on the landslide time accuracy. For Yosemite, landslides triggered 2 days after the $M_L = 6.1$ mainshock were most probably triggered by a $M_L = 6.2$ aftershock (see also Figure 4 and Table 3).

[33] The significance of these results is assessed by performing the same test on 100 randomized landslide catalogs. These catalogs were generated by keeping the original locations but using a random distribution in time. In order to preserve the distribution of daily rates of the original catalogs, we shuffled the number of events per day to destroy the temporal correlations between clusters. We find significant results up to $\Delta/L = 20$ for the three catalogs.

[34] Table 7 describes earthquakes which possibly triggered landslides and gives the characteristics of triggered landslides (number of events and distance from the earthquake). The smallest earthquake found to correlate with a landslide is a $M_L = 4.7$ event in Australia. The largest triggering distance is 500 km for a $M = 7.1$ earthquake in New Zealand. Note that the three largest Δ/L ($\Delta/L \sim 15$) are not associated with the largest magnitude earthquakes. Landslide increase at $t = 0$ to 2 days is due to a few earthquakes only and allow us to find the potential earthquake-triggered landslides, which were not all *a priori* labelled as such, especially the events with large Δ/L ratio. However, numerical modeling is needed to validate these landslides as earthquake triggered.

[35] Note that landslides are all spatially close to each other in the Yosemite catalog; therefore, when an earthquake with a given Δ/L is effective on a landslide (as three nearby Yosemite earthquakes were, see Table 7), it is also potentially effective on all the slopes of the Yosemite area. The fact that most landslides were not triggered by the three nearby Yosemite earthquakes but triggered later on indicates that Δ/L alone (and more generally any given threshold) is not sufficient to predict whether a landslide will occur or not. The geomorphological stage of the slope, i.e., its readiness for failure, should be included as well for earthquake-triggered landslide prediction.

Table 6. Landslide Daily Rate Distributions and Associated Power Laws[a]

Catalog Name	N	Exponent b	Lower Cutoff	p
New Zealand	1788	2.04 ± 0.11	1 ± 0.13	**0.26**
Yosemite	172	3.04 ± 0.21	1 ± 0.00	**0.93**
Grenoble	67			0.07
Val d'Arly	83			0
Australia	247	3.01 ± 0.21	1 ± 0.00	**0.42**
Wollongong	207	1.93 ± 0.20	1 ± 0.35	**0.37**

[a] N denotes the number of landslides, b the power law exponent and p the associated probability that the distribution follows the best power law fit. $p > 0.1$ (in bold) accepts power law as a possible description of the data. Standard deviation is calculated via a nonparametric bootstrap method (see *Clauset et al.* [2009] for details).

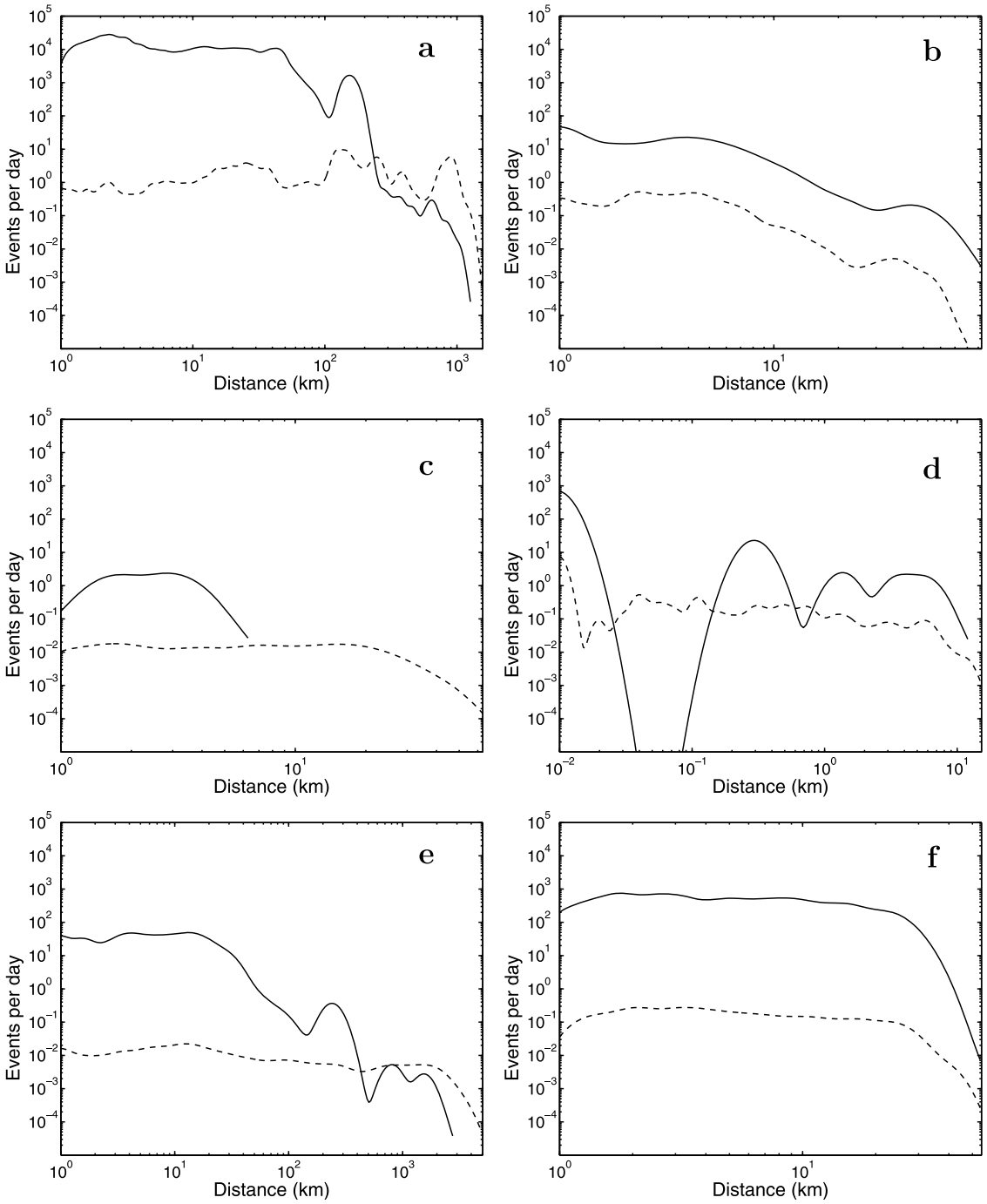

Figure 7. Distribution of inter-event distances for landslides occurring on the same day ($dt = 0$) (solid line) and landslides occurring at $dt > 1$ day (dashed line). (a) New Zealand, (b) Yosemite, (c) Grenoble, (d) Val d'Arly, (e) Australia, and (f) Wollongong. The distributions were computed using a lognormal kernel [*Izenman*, 1991]. A 0.01 km and a 1 km error were added to Val d'Arly distances and to New Zealand, Yosemite, Grenoble, Australia, and Wollongong distances, respectively.

[36] Finally, the effect of the 20 largest earthquakes on the long-term landsliding rate (200 days before and after large earthquake occurrences) is assessed for the different catalogs (Figure 12). No significant change of the landsliding rate is found except for the Wollongong catalog (less than 1% chance to find the same pattern when randomly selecting 20 earthquakes from the catalog and performing the same test).

4.3. Climate-Landslide Interactions

[37] The linear correlation coefficient r [e.g., *Press et al.*, 1992] measures the strength and the direction of a linear relationship between two variables. It is calculated between either the monthly binary or monthly entire landslide rate and the monthly weather variables, i.e., rainfall depth, number of rain days and temperature. r was also calculated for

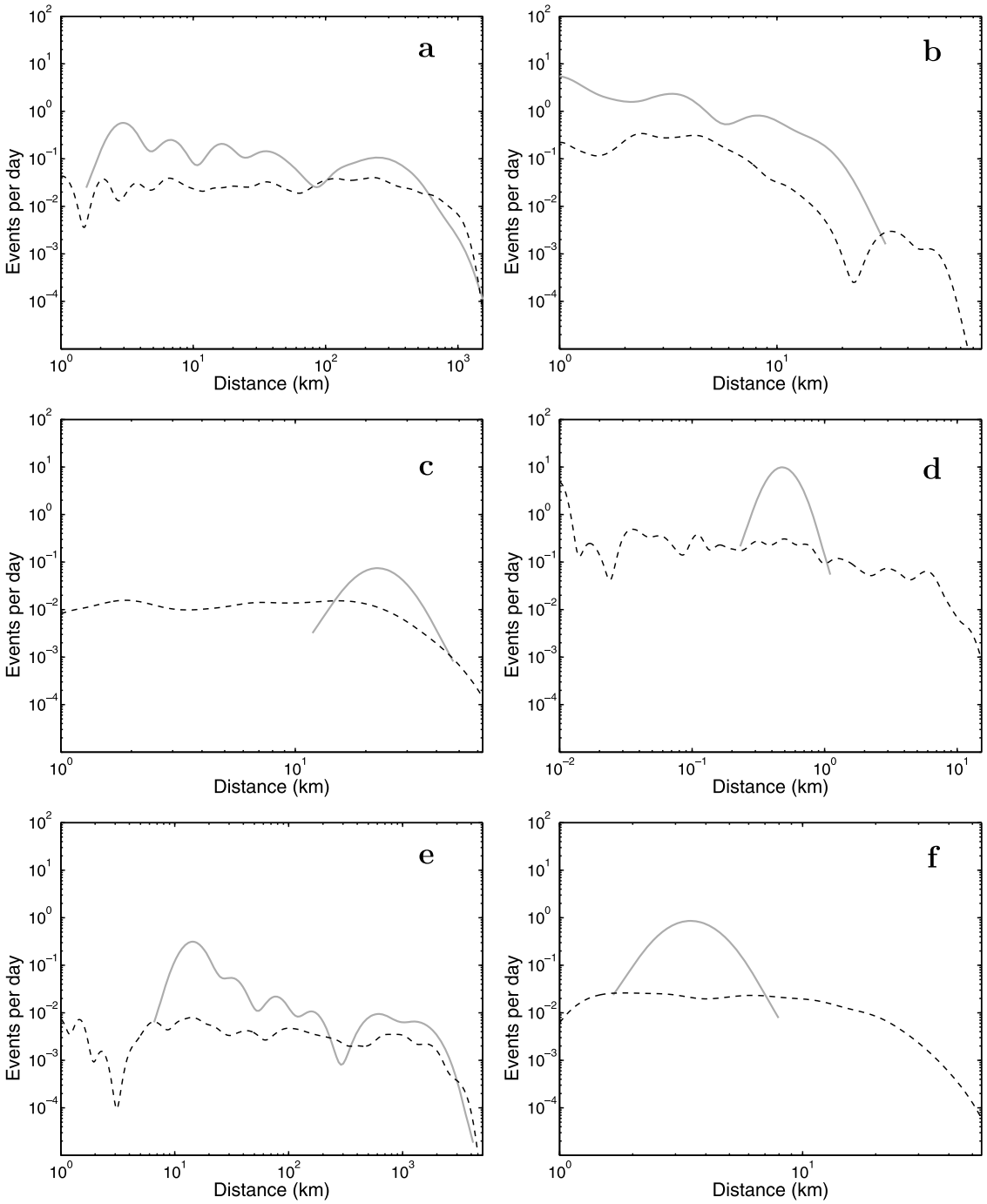

Figure 8. Same as Figure 7 but using the binary catalogs and comparing $dt = 1$ (solid gray line) with $dt > 1$ (dashed line).

daily variables. The r values obtained for daily variables are smaller than the r values obtained for monthly variables. This result indicates either that landslide time accuracy is not good enough or that landslide triggering is not only driven by daily rainfall. Notably, *Sidle and Ochiai* [2006] and *Crozier* [1999] showed the importance of the antecedent soil water status in the triggering of landslides and *Iverson* [2000] showed that different time scales existed for the triggering of rainfall induced landslides existed, depending on landslide type (shallow or deep seated).

[38] Table 8 gives the r values for the binary and entire catalogs. For New Zealand, Wollongong and Australia binary catalogs, the number of landslides per month correlates with the monthly rainfall depth and/or the monthly number of rainy days (Table 8). The New Zealand landslides are anticorrelated to the monthly maximum temperature (note that the New Zealand monthly temperatures and New Zealand monthly rainfall are not correlated: correlations of New Zealand landslides with temperatures and with rainfall are two independent results). The Grenoble landslides

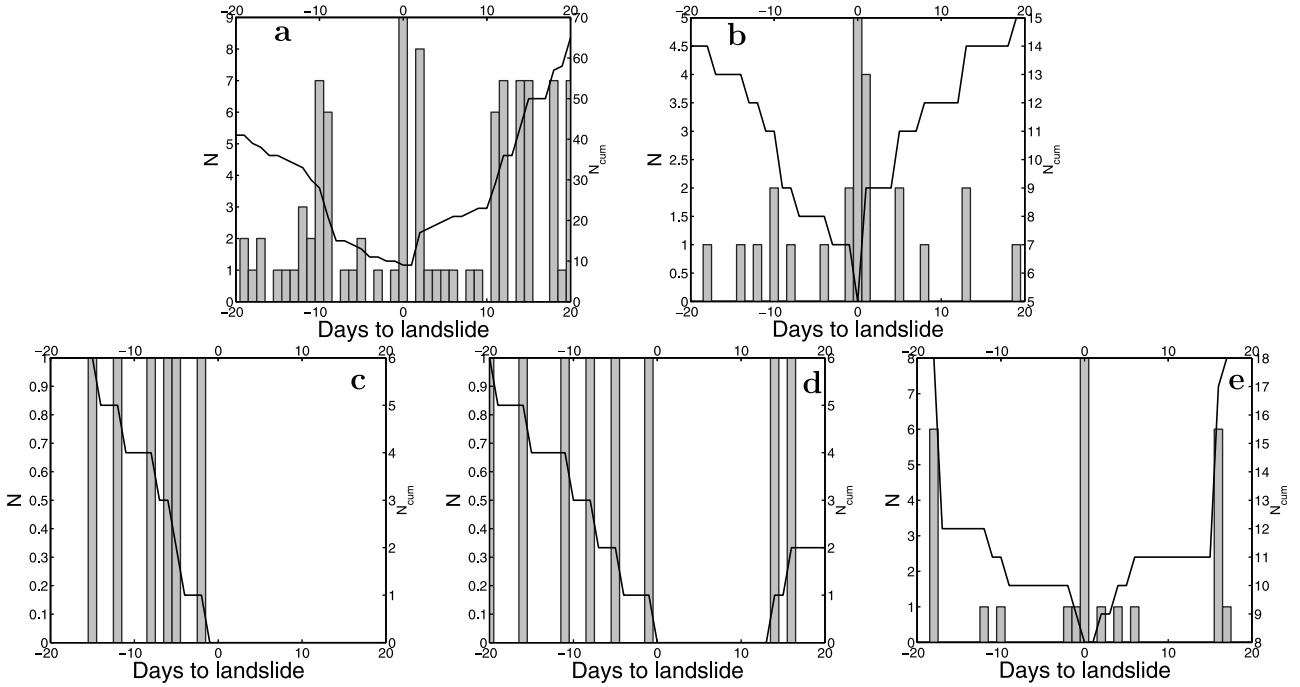

Figure 9. Stacked time series of binary landslide daily rates relative to the times of the 10 largest events. (a) New Zealand (volumes from 75,000 to 24 × 10^6 m^3), (b) Yosemite (volumes from 3200 to 6 × 10^5 m^3), (c) Grenoble (volumes from 800 to 20,000 m^3), (d) Val d'Arly (volumes from 600 to 4000 m^3), and (e) Australia (volumes from 300 to 2000 m^3). The black curves represent the cumulative number of events from $t = 0$ to $t = -20$ day and from $t = 0$ to $t = 20$ days before/after the large landslide occurrences. There are no volume data for the Wollongong catalog.

are anticorrelated with both the monthly minimum and maximum temperatures. The Val d'Arly landslides are correlated with both the monthly rainfall depth and the monthly number of rainy days. When using the full catalog for New Zealand, Wollongong and Australia areas, rather than the binary catalog, the correlation is weak or even nonsignificant. In contrast, for the Yosemite catalog, the correlation with rainfall depth is stronger for the full catalog than for the binary

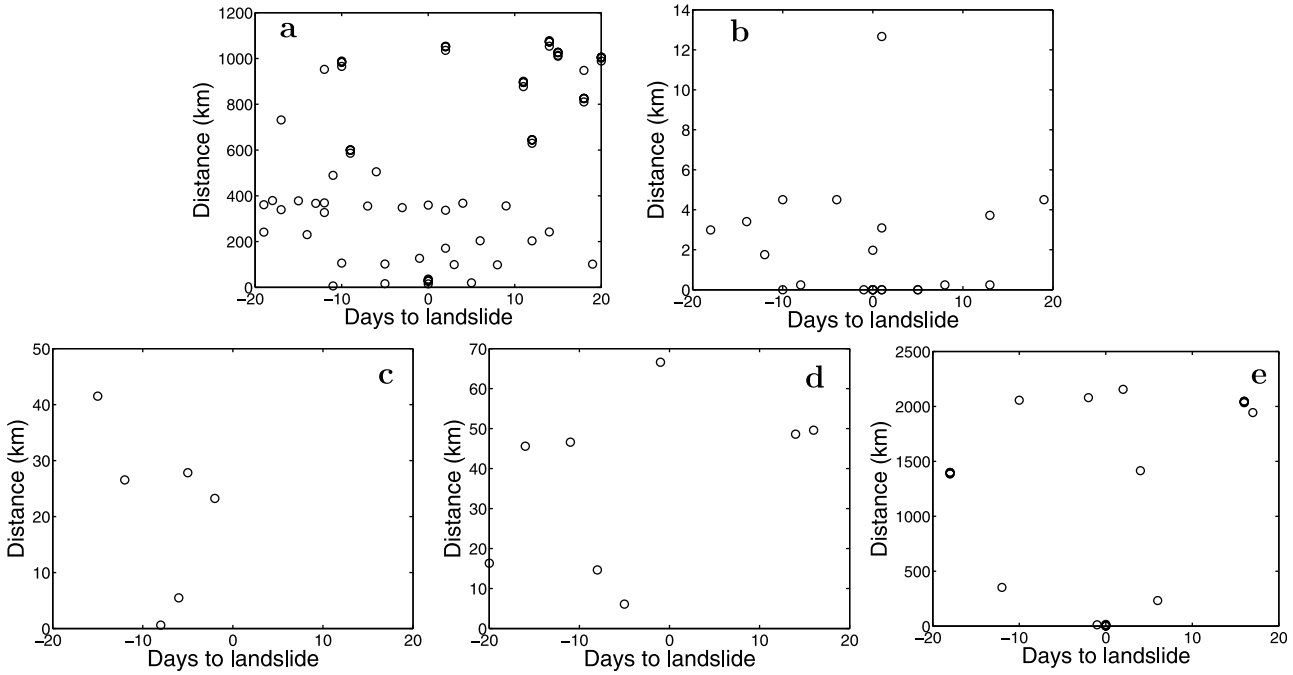

Figure 10. Distances between the 10 largest landslides and the landslides occurring 20 days before and after them. (a) New Zealand, (b) Yosemite, (c) Grenoble, (d) Val d'Arly, and (e) Australia.

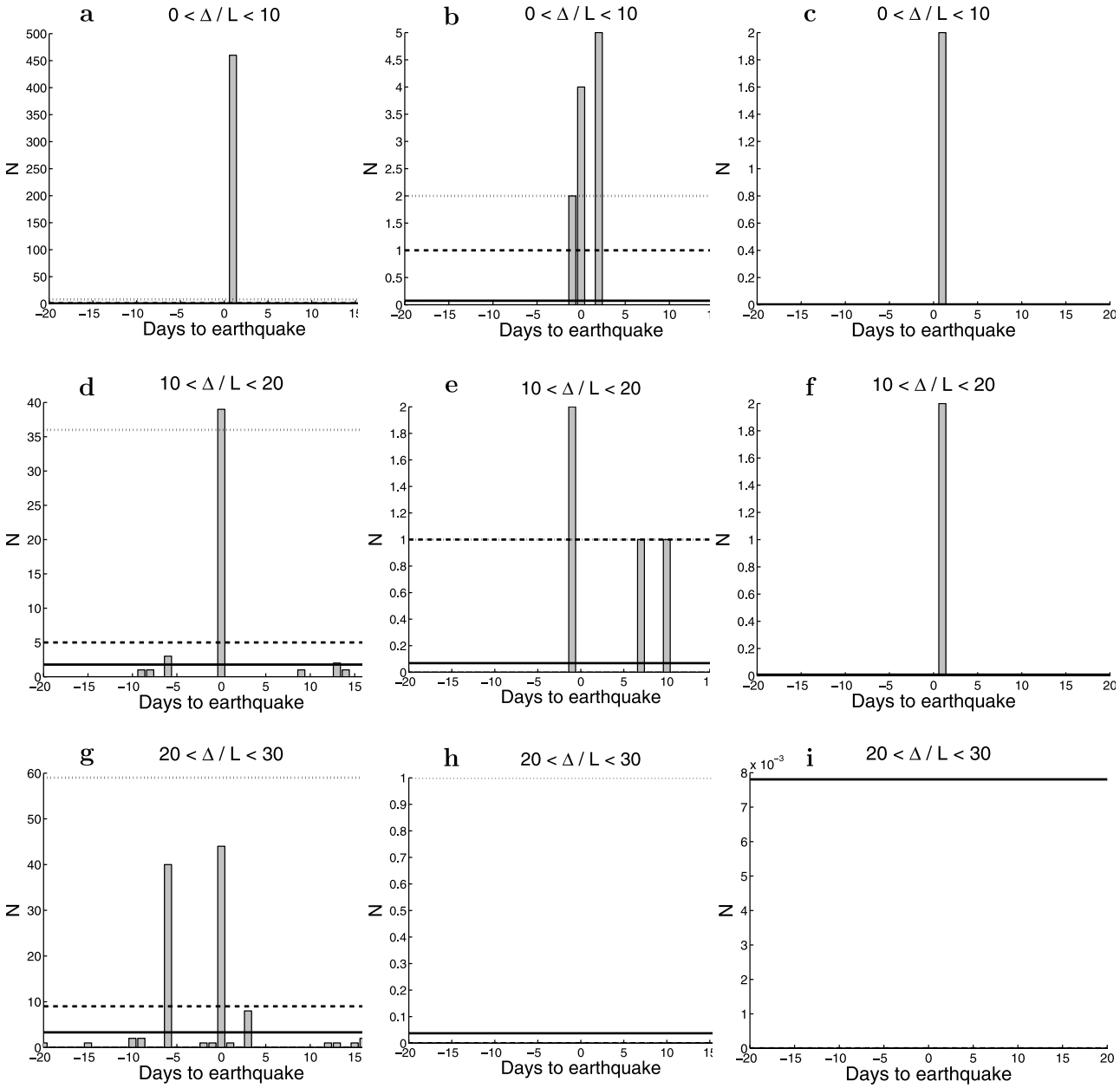

Figure 11. Stacked time series of landslides relative to earthquake occurrence times for New Zealand (Figures 11a, 11d, and 11g), Yosemite (Figures 11b, 11e, and 11h), and Australia (Figures 11c, 11f, and 11i) catalogs, for $0 < \Delta/L < 10$ (a–c) , $10 < \Delta/L < 20$ (d–f), and $20 < \Delta/L < 30$ classes (g–i). Solid line denotes the mean number of events from the randomized catalogs, the dashed line denotes the 95th centile, while the dotted line denotes the 99th centile.

catalog. For Grenoble and Val d'Arly catalogs r values for full or binary landslide rates are similar because these catalogs contain rarely more than one event per day. For the New Zealand catalog, some of the largest clusters of landslides were triggered by earthquakes. This additional forcing diminishes the correlation between weather variables and New Zealand landslide total rates, and may explain why the correlation is stronger with the binary catalog. For Australia and Wollongong, as few landslides were triggered by earthquakes (see Table 7) this does not explain the stronger correlation obtained for the binary catalog relatively to the full catalog. Other explanations may be the large variability of the number of triggered landslides for the same forcing and local fluctuations of the weather, so that binary catalogs (absence or presence of triggered landslides) are more correlated with our measures of the forcing, averaged over relatively large areas.

[39] There is an influence of temperature only for New Zealand and Grenoble catalogs, with a negative correlation between temperature (minimum and/or maximum) and landslide triggering. Low temperatures can favor freeze and thaw processes and can therefore produce rockfalls. Low tempera-

Table 7. List of Earthquakes in Each Area Which Have Potentially Triggered Landslides[a]

Catalog	Date of Earthquake	M_L	Number of Reported Landslides	Δ_{max} (km)	Δ_{max}/L	*a priori* Label
New Zealand	1 Nov 2000	6.2	1	16	1.48	Yes
New Zealand	22 Aug 2003	7.0	459	25–205	5.1	Yes
New Zealand	18 Jul 2004	5.1	52	30	16	Yes
New Zealand	22 Nov 2004	7.1	1	500	9.9	No
Yosemite	25 May 1980	6.1	4	75	7.9	Yes
Yosemite	27 May 1980	6.2	5	75	6.7	Yes
Yosemite	24 Oct 1990	5.8	4	60	11	Yes
Grenoble	None					
Val d'Arly	None					
Australia	28 Feb 1954	5.4	1	12	3.7	Yes
Australia	9 Mar 1973	5.5	1	63	16	Yes
Australia	2 Dec 1977	4.7	1	16	15	Yes
Australia	27 Dec 1989	5.7	1	14	2.7	Yes
Wollongong	None					

[a]Earthquake and landslide events at t = 0 to t = 2 days of Figure 11. Δ is the distance between earthquake hypocenter and triggered landslides and L is an estimate of the earthquake rupture length. The *a priori* label column indicates if landslides were *a priori* labelled as earthquake-triggered landslides in the catalog.

tures also reduce evapotranspiration, leading to wet slopes which are therefore particularly prone to landslides.

5. Discussion and Conclusions

[40] We have analyzed the properties of landslide triggering for six landslide inventories. These landslide catalogs span different scales in space (between 15 and 4000 km) and in time (from 4 to 25 years) and were gathered in different tectonic and climatic settings. The analysis of these catalogs allows us to investigate possible scale effects for landslide triggering. Obtaining catalogs robust in time, space and size, and not affected by anthropogenic factors, is a major issue when using landslide catalogs. Accordingly, landslide catalogs were selected over the time interval presenting a constant binary rate, excluding landslides with either a time inaccuracy larger than 2 days or no spatial location. Nevertheless, as data on volume are poor for most catalogs, a detection threshold above which catalogs are complete could not be defined, and therefore the catalogs were not corrected from their resolution (as performed by *Dussauge et al.* [2003]). This is an issue when comparing the different catalogs as it precludes the use of simple indexes such as landslide daily rates and densities. It is the reason why other indexes and tools are proposed to characterize and compare landslide triggering in different settings.

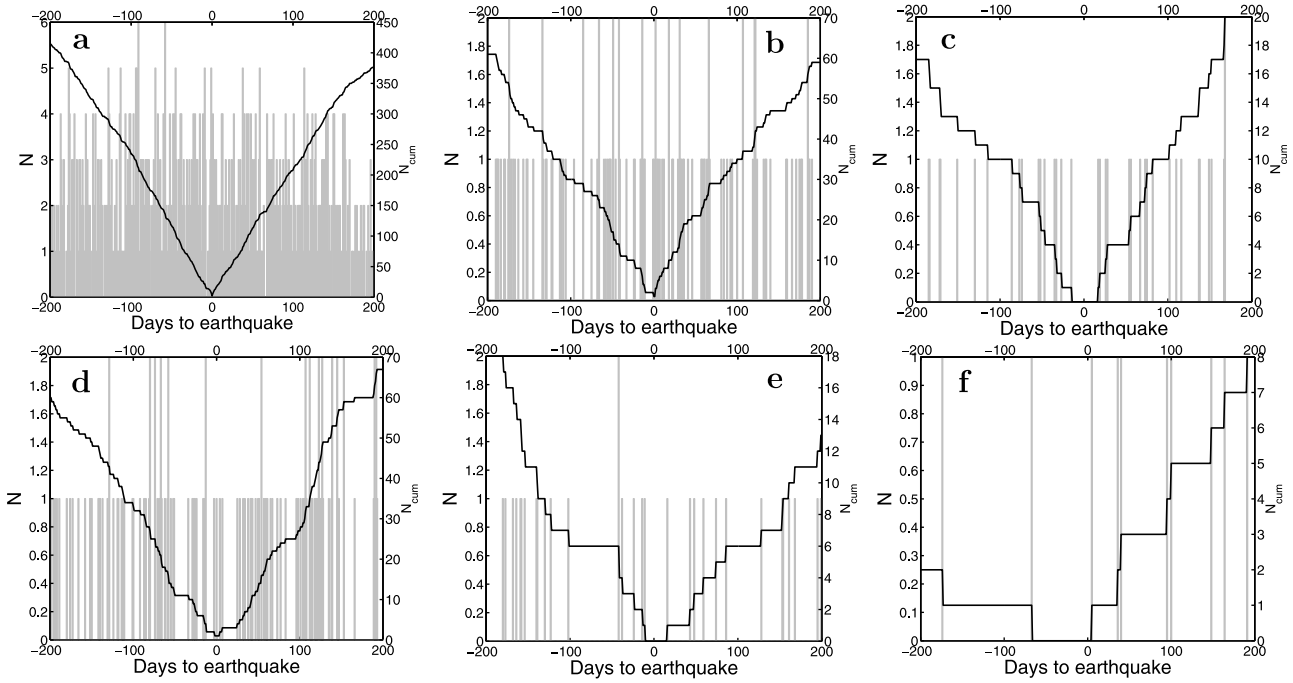

Figure 12. Stacked time series of binary landslide daily rates relative to the times of the 20 largest earthquakes. (a) New Zealand, (b) Yosemite, (c) Grenoble, (d) Val d'Arly, (e) Australia, and (f) Wollongong. The black curves represent the cumulative number of events from $t = 0$ to $t = -200$ day and from $t = 0$ to $t = 200$ days before/after the large earthquake occurrences.

Table 8. Monthly Correlation Between Binary or Full Landslide Rates and Weather (Rain, Rain Days, Temperature)[a]

Catalog	Rain	Number of Rain Days	Minimum Temperature	Maximum Temperature	Mean Temperature
			Binary		
New Zealand	**0.35** (0.03)	**0.42** (<0.01)	−0.29 (0.06)	**−0.35** (0.03)	No data
Wollongong	**0.62** (<0.01)	**0.26** (<0.01)	0.08 (0.33)	−0.02 (0.85)	No data
Australia	**0.32** (<0.01)	No data	No data	No data	0.11 (0.20)
Yosemite	0.08 (0.16)	No data	0.08 (0.18)	0.07 (0.26)	No data
Val d'Arly	**0.15** (0.02)	**0.12** (0.05)	0.04 (0.49)	0 (0.95)	No data
Grenoble	0.11 (0.10)	0.06 (0.34)	**−0.14** (0.03)	**−0.16** (0.02)	No data
			Full		
New Zealand	0.27 (0.09)	0.22 (0.16)	−0.03 (0.88)	−0.06 (0.73)	No data
Wollongong	**0.47** (<0.01)	0.14 (0.10)	−0.04 (0.66)	−0.09 (0.30)	No data
Australia	**0.29** (<0.01)	No data	No data	No data	0.17 (0.06)
Yosemite	**0.16** (<0.01)	No data	0.06 (0.33)	0.03 (0.60)	No data
Val d'Arly	**0.21** (<0.01)	**0.13** (0.03)	0.01 (0.83)	−0.04 (0.51)	No data
Grenoble	0.12 (0.07)	0.06 (0.34)	**−0.15** (0.02)	**−0.17** (0.01)	No data

[a]If the significance of correlation (given within brackets) is less than 0.05, the correlation is considered as significant, and the correlation coefficient value is in bold.

[41] Landslide time series show large daily fluctuations of landslide rate (Figure 2). Figures 3 and 4 also show clusters of landslides in time and space, evidencing triggering by rain and earthquakes. The response of the slopes to earthquakes and rainfall seems to be variable in space and time, most probably due to the heterogeneity of the upper crust (different geology, geomorphology) as well as heterogeneous external loadings (temperature, soil moisture, vegetation, earthquake or rainfall characteristics).

[42] Landslides are strongly correlated in time, even when using binary catalogs to reduce short-time clustering. The inter-event time distributions of binary catalogs depart from a Poisson process for inter-event times larger than a value t_r, which varies between 30 and 250 days for the different catalogs. For inter-event times larger than t_r, the number of large inter-event times is higher than expected for uniformly distributed times. This deviation from a Poisson process for $t > t_r$ may be due to the seasonal variations of climate: landslides are less frequent (or absent) during the dry season, which leads to larger inter-event times than expected from a Poisson distribution.

[43] Landslide daily rates follow a power law distribution for rates between 1 and 1000 events per day, for the New Zealand, Yosemite, Australia and Wollongong catalogs. A possible deviation from a power law is found above 10 landslides per day for the New Zealand, Australia and Wollongong catalogs (Figure 6 and section 3.4). The fact that landslide daily rate distributions can be fitted by a power law implies that there is no characteristic scale for daily rates. It suggests that the same mechanisms are driving both the large clusters of landslides and the isolated events. Because the largest clusters are known to have been triggered by rainfall or earthquakes, this suggests that isolated events may also have been triggered by these forcings. As there is no obvious trigger for the isolated landslides, our results suggest that the delay between a possible trigger and a landslide may be longer than a few days. Indeed, delays between a landslide and its trigger larger than a few days have been suggested recently in several case studies. As examples, *Lin et al.* [2008] showed that the Chi-Chi earthquake raised the landsliding rates of the epicentral region above the pre-Chi-Chi rate, up to 5 years after the occurrence of the Chi-Chi mainshock. For rainfall triggering, *Helmstetter and Garambois* [2010] showed that, for a large rockslide in the French Alps, rainfall can trigger small rockslides up to 5 days after the maximum of rainfall intensity. The power law distribution of landslide daily rates may be driven either by the direct response to triggers, since these latter are known to be power law distributed in size [e.g., *Gutenberg and Richter*, 1956] for earthquakes and [e.g., *Peters et al.*, 2001; *Peters and Christensen*, 2002] for rainfall depth, or by the heterogeneous response of the brittle crust to external forcings.

[44] For the Yosemite, Val d'Arly and Wollongong catalogs, the maximum correlation distance between landslides occurring on the same day corresponds to the spatial extent of the studied catalog; therefore it is only a lower estimate of the maximum triggering distance. They are equal to 50, 10 and 30 km for the Yosemite, Val d'Arly and Wollongong catalogs, respectively. For the New Zealand, Australia and Grenoble catalogs, the maximum correlation distances are equal to 50 (up to 200), 30 (up to 400) and 3 km, respectively. These length scales are a measure of the combined effect of the trigger intensity and of the slope susceptibility. For events occurring 1 day from each other, the spatial extent of landslide triggering is roughly similar to the size of the sampled area for New Zealand and Australia, whereas it is roughly equal to 10 km for Yosemite and absent for the other catalogs.

[45] We found no evidence for direct interactions between landslides for any of the six catalogs. Indeed, when looking at the landslide rates before and after the 10 largest landslides, we found no systematic change in landslide activity before or after these large events. The French Alps catalogs showed a significant increase in landslide rate before the largest landslides, the New Zealand catalog showed a significant increase in landslide rate after the largest landslides, while the Yosemite and Australia catalogs did not show any particular trend.

[46] Triggering of landslides by earthquakes was observed in New Zealand, Yosemite and Australia, which are the areas with the largest seismicity rates. Significant triggering by earthquakes is found for distances up to twenty times the earthquake fault length. However, only a few earthquakes did trigger landslides (Table 7). We did not find any evidence for triggering by small $M < 4$ earthquakes. There are only a few studies in the literature on landslides triggered by $M < 4$

Table 9. Synthesis of Landslide Triggering Characteristics for the Six Studied Areas, From the Most Efficient Landslide Triggering Area (New Zealand) to the Least Efficient One (Grenoble)

Catalog	New Zealand	Wollongong	Australia	Yosemite	Val d'Arly	Grenoble
η (binary)	2.3 (1.5)	3.4 (1.3)	1.8 (1.3)	2.1 (1.8)	1.5 (1.4)	1.2 (1.2)
Daily rate power law exponent	2.04	1.93	3.01	3.04		
Maximum distance of correlation (km)	0–50 (up to 200)	0–30	0–20 (up to 400)	0–40	0–10	2–3
Triggered landslides, $dt = 1$	+	−	+	+	−	−
Correlation with earthquakes	++	−	+	+	−	−
Correlation with rainfall	++	++	+	−	+	−
Correlation with temperature	+	−	−	−	−	+

earthquakes. Results from these studies are often ambiguous, with no definite effect of $M < 4$ earthquakes on landslide triggering. *Del Gaudio et al.* [2000] studied the influence of a sequence of small $M \leq 3.6$ earthquakes on a less than 20 km away landslide in Vadoncello (Southern Italy). They found that it was dubious whether the seismic accelerations generated within the landslide were sufficient to activate mass movements and whether the effect of repeated shocks on hydrogeological conditions could explain the time delay observed between seismic and landslide accelerations. *Sassa et al.* [2007] argued that the $M_s = 2.6$ earthquake which occurred on the same day as the 22 km distant Leyte landslide (Philippines), was the cause of the landslide failure, which also occurred 5 days after a heavy rainfall. *Walter and Joswig* [2008] suggested that local (≈10 km distant) $M \approx 2$ earthquakes may have caused stress relief within the sliding body and triggered fracture initiation or growth within the Heumoes slope, Voralberg Alps, Austria.

[47] We find an increase of the landsliding rate in the 200 days after the 20 largest earthquakes in the Wollongong area (Figure 12), while no increase is found for the 5 other catalogs. Such a landslide rate increase was also observed in the Chenyoulan catchment, Taiwan: *Lin et al.* [2008] showed that in the 6 years after the Chi-Chi earthquake, typhoons have triggered large numbers of landslides at 13 times the preearthquake rate.

[48] Another well known mechanism for landslide triggering is climatic processes. To assess the influence of weather on landslide triggering, we have analyzed the correlation between landsliding rate and meteorological data. In New Zealand, Val d'Arly, Australia and Wollongong, the binary monthly landslide catalogs correlate with both the monthly rainfall depth and the monthly number of rainy days (Table 8). Grenoble landslides are anticorrelated with both the monthly minimum and maximum temperatures, whereas New Zealand landslides are only anticorrelated with the maximum temperatures (Table 8). In Yosemite, the full monthly landslide catalog correlated with monthly rainfall, while the binary monthly landslide catalog did not. The difference in correlation with climate between binary and full catalogs is not clear. In New Zealand, numerous landslides are triggered by earthquakes so this can weaken the correlation with climate. Thus looking at binary catalogs allows us to reduce this bias. For the other areas, as just a few landslides were triggered by earthquakes, this does not explain the stronger correlation obtained for the binary catalog than for the full catalog. Other explanations may be the large variability of the number of triggered landslides for the same forcing, and local fluctuations of the weather, so that binary catalogs (absence or presence of triggered landslides) are more correlated with our measures of the forcing, averaged over relatively large areas. The correlation of landslide activity with rainfall depth and number of rainy days confirms the role of rainfall in landslide triggering, due to pore pressure increase [e.g., *Sidle and Ochiai*, 2006]. The anticorrelation of landslide activity with temperatures emphasizes the role of temperature in landslide triggering, through frost weathering processes, as proposed by *Matsuoka and Murton* [2008]. Further, low temperature reduces evapotranspiration, and therefore increase soil moisture, which itself drives slopes susceptibility [see also *Glade et al.*, 2005].

[49] The intensity of clustering in time and space, as well as the correlation between landslide and climate or landslide and seismicity, can give information on landslide triggering. Landslide triggering depends both on the susceptibility of the slopes and on the applied forcing [see also *Vahrson*, 1994; *Dilley et al.*, 2005]. From our study, we find that New Zealand presents the most efficient landslide triggering (high clustering in time and space and strong interactions of landslides with seismicity and climate) and Grenoble presents the least efficient one (low clustering in time and space and weak landslide interactions with seismicity and climate). Nevertheless, it appears difficult to compare and classify all catalogs. Comparing New Zealand and Grenoble catalogs, the clustering is much stronger in the first case; as quantified by η value, daily rate distribution is power law for New Zealand and close to a Poisson distribution for Grenoble; the triggering distance is up to 200 km for New Zealand and less than 3 km for Grenoble; and the correlation with the weather and earthquake forcings is larger for New Zealand than for Grenoble (see Table 9).

[50] **Acknowledgments.** The authors are supported by EC TRIGS project. L.T. is funded by the French Ministry of Research, EGIDE, and EXPLORA'DOC scholarships. The authors are very thankful to Grant Dellow (GNS), Gerald Wieczoreck (USGS), Monica Osuchowski (Geoscience Australia), Phil Flentje (University of Wollongong), and Service de Restauration des terrains en montagne for the landslide databases. For the weather databases, the authors thank NIWA, Météo France, NOAA, and the Bureau of Meteorology. For the earthquake databases, the authors thank GNS, USGS, François Thouvenot (SISMALP), and Mark Leonard (Geoscience Australia). This paper benefited considerably from reviews of Tim Davies, the Associate Editor, and an anonymous reviewer.

References

Aki, K. (1965), Maximum likelihood estimate of b in the formula log N = a−bM and its confidence limits, *Bull. Earthquake Res. Inst. Univ. Tokyo*, *43*, 237–239.

Bonnet, E., O. Bour, N. E. Odling, P. Davy, I. Main, P. Cowie, and B. Berkowitz (2001), Scaling of fracture systems in geological media, *Rev. Geophys.*, *39*, 347–383, doi:10.1029/1999RG000074.

Brooks, S. M., M. J. Crozier, N. J. Preston, and M. G. Anderson (2002), Regolith stripping and the control of shallow translational hillslope failure: Application of a two-dimensional coupled soil hydrology-slope stability model, Hawke's Bay, New Zealand, *Geomorphology*, *45*(3–4), 165–179.

Brooks, S. M., M. J. Crozier, T. W. Glade, and M. G. Anderson (2004), Towards establishing climatic thresholds for slope instability: Use of a physically-based combined soil hydrology-slope stability model, *Pure Appl. Geophys.*, *161*(4), 881–905.

Caine, N. (1980), The rainfall intensity-duration control of shallow landslides and debris flows, *Geogr. Ann.*, *62*(1–2), 23–27.

Clauset, A., C. R. Shalizi, and M. E. J. Newman (2009), Power law distributions in empirical data, *SIAM Review*, *51*, 661–703, doi:10.1137/070710111.

Crozier, M. J. (1996), The climate-landslide couple: A Southern Hemisphere perspective, *Paleoclimate Res.*, *19*, 329–350.

Crozier, M. J. (1999), Prediction of rainfall-triggered landslides: A test of the antecedent water status model, *Earth Surf. Processes Landforms*, *24*(9), 825–833.

Del Gaudio, V., R. Trizzino, G. Calcagnile, A. Calvaruso, and P. Pierri (2000), Landsliding in seismic areas: The case of the Acquara-Vadoncello landslide (southern Italy), *Bull. Eng. Geol. Environ.*, *59*(1), 23–37.

Dilley, M., R. S. Chen, and U. Deichmann (2005), *Natural Disaster Hotspots: A Global Risk Analysis*, World Bank Publ., Washington, D. C.

Dixon, T. H., M. Miller, F. Farina, H. Wang, and D. Johnson (2000), Present-day motion of the Sierra Nevada block and some tectonic implications for the Basin and Range province, North American Cordillera, *Tectonics*, *19*(1), 1–24.

Dussauge, C., A. Helmstetter, J. R. Grasso, D. Hantz, P. Desvarreux, M. Jeannin, and A. Giraud (2002), Probabilistic approach to rock fall hazard assessment: Potential of historical data analysis, *Nat. Hazards Earth Syst. Sci.*, *2*, 15–26.

Dussauge, C., J. R. Grasso, and A. Helmstetter (2003), Statistical analysis of rockfall volume distributions: Implication for rockfall dynamics, *J. Geophys. Res.*, *108*(B6), 2286, doi:10.1029/2001JB000650.

Felzer, K. R., and E. E. Brodsky (2006), Decay of aftershock density with distance indicates triggering by dynamic stress, *Nature*, *441*(7094), 735–738.

Fitzsimons, S. J., and H. Veit (2001), Geology and geomorphology of the European Alps and the Southern Alps of New Zealand, *Mt. Res. Dev.*, *21*(4), 340–349.

Flentje, P., and R. N. Chowdhury (2005), Managing landslide hazards on the Illawarra escarpment, in *Proceedings of the GeoQuest Symposium on Planning for Natural Hazards - How can we mitigate the impacts?*, edited by J. Morrison, pp. 65–78, GeoQuest Res. Centre, Wollongong, N. S. W., Australia.

Flentje, P., D. Stirling, and R. N. Chowdhury (2007), Landslide susceptibility and hazard derived from a landslide inventory using data mining - An Australian case study, paper presented at First North American Landslide Conference, Landslides and Society: Integrated Science, Engineering, Management, and Mitigation, Vail, Colo., 3–8 June.

Frayssines, M., and D. Hantz (2006), Failure mechanisms and triggering factors in calcareous cliffs of the Subalpine Ranges (French Alps), *Eng. Geol.*, *86*(4), 256–270.

Glade, T. (1998), Establishing the frequency and magnitude of landslide-triggering rainstorm events in New Zealand, *Environ. Geol.*, *35*(2), 160–174.

Glade, T. (2000), Applying probability determination to refine landslide-triggering rainfall thresholds using an empirical antecedent daily rainfall model, *Pure Appl. Geophys.*, *157*(6), 1059–1079.

Glade, T., M. Anderson, and M. J. Crozier (2005), *Landslide Hazard and Risk*, Wiley, Chichester, U. K.

Gruner, U. (2008), Climatic and meteorological influences on rockfall and rockslides, paper presented at 11th Interpraevent Congress 2008 Protection of Populated Territories From Floods, Debris Flows, Mass Movements and Avalanches, Dornbirn, Austria, 26–30 May.

Gutenberg, B., and C. F. Richter (1956), Earthquake magnitude, intensity, energy, and acceleration, *Bull. Seismol. Soc. Am.*, *46*(2), 105–145.

Guzzetti, F., S. Peruccacci, M. Rossi, and C. P. Stark (2007), Rainfall thresholds for the initiation of landslides in central and southern Europe, *Meteorol. Atmos. Phys.*, *98*(3), 239–267.

Helmstetter, A., and S. Garambois (2010), Seismic monitoring of Séchilienne Rockslide (French Alps): Analysis of seismic signals and their correlation with rainfalls, *J. Geophys. Res.*, *115*, F03016, doi:10.1029/2009JF001532.

Hufschmidt, G., and M. J. Crozier (2008), Evolution of natural risk: Analysing changing landslide hazard in Wellington, Aotearoa/New Zealand, *Nat. Hazards*, *45*, 255–276.

Iverson, R. M. (2000), Landslide triggering by rain infiltration, *Water Resour. Res.*, *36*(7), 1897–1910.

Izenman, A. J. (1991), Recent developments in nonparametric density estimation, *J. Am. Stat. Assoc.*, *86*, 205–224.

Keefer, D. K. (1984), Landslides caused by earthquakes, *Geol. Soc. Am. Bull.*, *95*(4), 406–421.

Keefer, D. K. (2002), Investigating landslides caused by earthquakes–A historical review, *Surv. Geophys.*, *23*, 473–510.

Lemarchand, N., and J. R. Grasso (2007), Interactions between earthquakes and volcano activity, *Geophys. Res. Lett.*, *34*, L24303, doi:10.1029/2007GL031438.

Leonard, M. (2008), One hundred years of earthquake recording in Australia, *Bull. Seismol. Soc. Am.*, *98*(3), 1458–1470.

Lin, G. W., H. Chen, N. Hovius, M. J. Horng, S. Dadson, P. Meunier, and M. Lines (2008), Effects of earthquake and cyclone sequencing on landsliding and fluvial sediment transfer in a mountain catchment, *Earth Surf. Processes Landforms*, *33*(9), 1354–1373.

Marzocchi, W., and L. Zaccarelli (2006), A quantitative model for the time-size distribution of eruptions, *J. Geophys. Res.*, *111*, B04204, doi:10.1029/2005JB003709.

Matsuoka, N., and J. Murton (2008), Frost weathering: Recent advances and future directions, *Permafrost Periglacial Processes*, *19*, 195–210.

Miner, A. S., P. Flentje, C. Mazengrab, J. M. Selkirk-Bell, and P. Dalhaus (2008), Some geomorphological techniques used in constraining the likelihood of landsliding – selected Australian examples, paper presented at 10th International Symposium on Landslides and Engineered Slopes, Joint Tech. Comm. on Landslides and Eng. Slopes, Xi'an, China.

Ogata, Y., and K. Katsura (1993), Analysis of temporal and spatial heterogeneity of magnitude frequency distribution inferred from earthquake catalogs, *Geophys. J.*, *113*(3), 727–738.

Peters, O., and K. Christensen (2002), Rain: Relaxations in the sky, *Phys. Rev. E*, *66*(3), 036120–036129.

Peters, O., C. Hertlein, and K. Christensen (2001), A complexity view of rainfall, *Phys. Rev. Lett.*, *88*(1), 018701–018705.

Press, W. H., B. Flannery, S. A. Teukolsky, and W. T. Vetterling (1992), *Numerical Recipes in C: The Art of Scientific Computing*, 2nd ed., Cambridge Univ. Press, New York.

Sandersen, F., S. Bakkehoi, E. Hestnes, and K. Lied (1996), The influence of meteorological factors on the initiation of debris flow, rockfall, rockslides and rockmass stability, in *Proceedings of the Seventh International Symposium on Landslides, Trondheim*, vol. 1, edited by K. Senneset, pp. 97–114, A. A. Balkema, Rotterdam, Neth.

Sassa, K., H. Fukuoka, F. Wang, and G. Wang (Eds.) (2007), Landslides induced by a combined effect of earthquake and rainfall, in *Progress in Landslide Science*, pp. 193–207, Springer, Berlin.

Sidle, R. C., and H. Ochiai (2006), *Landslides: Processes, Prediction, and Land Use*, *Water Resour. Monogr. Ser.*, vol. 18, 312 pp., AGU, Washington, D. C.

Tatard, L. (2010), Statistical analysis of triggered landslides: Implications for earthquake and weather controls, Ph.D. thesis, Université Joseph Fourier, Grenoble, France.

Traversa, P., and J. R. Grasso (2009), Brittle creep damage as the seismic signature of dyke propagations within basaltic volcanoes, *Bull. Seismol. Soc. Am.*, *99*(3), 2035–2043.

Vahrson, W. G. (1994), Macrozonation methodology for landslide hazard determination, *Bull. Assoc. Eng. Geol.*, *31*, 49–58.

Walter, M., and M. Joswig (2008), Seismic monitoring of fracture processes from a creeping landslide in the Vorarlberg Alps, *Geophys. Res. Abstr.*, *10*, 09212.

Wells, D. L., and K. J. Coppersmith (1994), New empirical relationships among magnitude, rupture length, rupture width, rupture area, and surface displacement, *Bull. Seismol. Soc. Am.*, *84*(4), 974–1002.

Whipple, K. X. (2009), The influence of climate on the tectonic evolution of mountain belts, *Nat. Geosci.*, *2*(2), 97–104.

Wieczorek, G. F., and J. B. Snyder (2004), Historical rock falls in Yosemite National Park, California, *U.S. Geol. Surv. Open File Rep.*, *03-491*.

S. Garambois, J. R. Grasso, A. Helmstetter, and L. Tatard, Laboratoire de Géophysique Interne et de Tectonophysique, Université Joseph Fourier, BP 53, F-38041 Grenoble Cedex 9, France. (ltatard@obs.ujf-grenoble.fr)